Numerical Simulation on Spatial Curves for Distributed Parameter Propagation Processes

Vlad Mureşan, Iulia Clitan, Tiberiu Coloşi, Mihail Abrudean, Mihaela-Ligia Ungureşan, and Andrei Clitan

***Abstract*—The paper is referring to distributed parameter propagation phenomena, in relation to the Cartesian coordinate axes (0*p*;0*q*;0*r*). The analogical model of the propagation phenomenon is expressed through a partial differential equation of second (II) order, associated to each coordinate axis. The numerical integration is based on the matrix of partial derivatives of the state vector (M_{pdx}), that uses approximating solutions for the calculations start. The numerical simulation of the propagation phenomenon follows parametrical spatial curves predetermined in relation to time (*t*), respectively $p = p(t)$, $q = q(t)$, and $r = r(t)$, in the period $t_0 \le t \le t_f$. The examples run on the computer are referring to identical or different propagation parameters in relation to the three Cartesian coordinate axes. The numerical simulation evolves after spatial curves in form of a spiral, which encloses significantly the evolution of the studied phenomenon. Some references are made on the applicability of the elaborated programs, for chemical, metallurgical, pollution processes etc.**

***Index Terms*—Partial differential equations (PDEs), analogical modeling, numerical simulation, matrix of partial derivatives of the state vector, thermal propagation, structure parameters, approximating solutions.**

I. Introduction

In Fig. 1, a propagation phenomenon (for example of the temperature) $y_{0000}(t,p,q,r)$, oriented on the Cartesian coordinate axes (0*p*; 0*q*; 0*r*) is formally presented, where the propagation sources are disposed in the origin of these coordinate axes. It is considered that the propagation phenomenon is different, in relation to each from the three coordinate axes [1]-[3]. With the increasing of the propagation time, from (t_0), (t_1), (t_2).., to the final time (t_f), and of the propagation distances on each axis, respectively (p_0, p_1, p_2,..., p_f), (q_0, q_1, q_2,..., q_f), and (r_0, r_1, r_2,..., r_f), the propagation on each axis will progressively decrease, respectively $y_{00P}(t_i, p_i)$, $y_{00Q}(t_i, q_i)$ and $y_{00R}(t_i, r_i)$, for $(i = 0, i = 1, i_2,..., i_f)$, presenting negligible values at $y_{00P}(t_f, p_f)$, $y_{00Q}(t_f, q_f)$ and $y_{00R}(t_f, r_f)$.

The analogical model of the propagation phenomenon on each axis, is considered that it can be expressed through partial differential equations (PDE) of II order (*t*,....), respectively [4]-[7]: PDE II (*t*, *p*) for (0*p*) axis, PDE II (*t*, *q*) for (0*q*) axis, PDE II (*t*, *r*) for (0*r*) axis, as it is shown in Table I.

Manuscript received May 20, 2018; revised June 19, 2018.

The authors are with Technical University of Cluj-Napoca, Cluj-Napoca, 400114, Romania (e-mail: Vlad.Muresan@aut.utcluj.ro, Iulia.Inoan@aut.utcluj.ro, Tiberiu.Coloşi@aut.utcluj.ro, Mihail.Abrudean@aut.utcluj.ro, Mihaela.Ungureşan@chem.utcluj.ro, Andrei.Clitan@infra.utcluj.ro).

I.

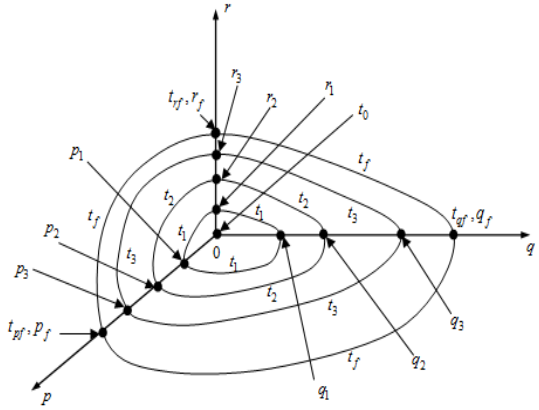

Fig. 1. Example of propagation phenomenon oriented on the Cartesian coordinate axes.

TABLE I: The Model of the Propagation Phenomenon on Each Axis

Axes	PARAMETERS / MEDIUM	t_{fP}	μ_{TP}	λ_{TP}	T_{1P}	T_{2P}	p_f	μ_P	λ_P	P_1	P_2
0*p* Axis	HOMOGENOUS	10	4	1.5	1	1.5	10	4	1.5	1	1.5
	INHOMOGENEOUS	10	4	1.5	1	1.5	10	4	1.5	1	1.5
	PDE (t,p)	$a_{00P}\cdot y_{00P}+a_{10P}\cdot y_{10P}+a_{20P}\cdot y_{20P}+a_{01P}\cdot y_{01P}+a_{02P}\cdot y_{02P}+a_{11P}\cdot y_{11P} = K_{yP}\cdot(\varphi_{0.00P}\cdot u_{0P}+\varphi_{1.00P}\cdot u_{1P}+\varphi_{2.00P}\cdot u_{2P})$									
	$\tilde{y}_{00P}(t,p)$	$K_{yP}\cdot(1-\frac{T_{1P}}{T_{1P}-T_{2P}}\cdot e^{-\frac{t}{T_{1P}}}-\frac{T_{2P}}{T_{2P}-T_{1P}}\cdot e^{-\frac{t}{T_{2P}}})\cdot(\frac{P_1}{P_1-P_2}\cdot e^{-\frac{p}{P_1}}-\frac{P_2}{P_2-P_1}\cdot e^{-\frac{p}{P_1}})$									
0*q* Axis	PARAMETERS / MEDIUM	t_{fQ}	μ_{TQ}	λ_{TQ}	T_{1Q}	T_{2Q}	q_f	μ_Q	λ_Q	Q_1	Q_2
	HOMOGENOUS	10	4	1.5	1	1.5	10	4	1.5	1	1.5
	INHOMOGENEOUS	18	4	1.25	2	2.5	18	4	1.25	2	2.5
	PDE (t,q)	$a_{00Q}\cdot y_{00Q}+a_{10Q}\cdot y_{10Q}+a_{20Q}\cdot y_{20Q}+a_{01Q}\cdot y_{01Q}+a_{02Q}\cdot y_{02Q}+a_{11Q}\cdot y_{11Q} = K_{yQ}\cdot(\varphi_{0.00Q}\cdot u_{0Q}+\varphi_{1.00Q}\cdot u_{1Q}+\varphi_{2.00Q}\cdot u_{2Q})$									
	$\tilde{y}_{00Q}(t,q)$	$K_{yQ}\cdot(1-\frac{T_{1Q}}{T_{1Q}-T_{2Q}}\cdot e^{-\frac{t}{T_{1Q}}}-\frac{T_{2Q}}{T_{2Q}-T_{1Q}}\cdot e^{-\frac{t}{T_{2Q}}})\cdot(\frac{Q_1}{Q_1-Q_2}\cdot e^{-\frac{q}{Q_1}}-\frac{Q_2}{Q_2-Q_1}\cdot e^{-\frac{q}{Q_1}})$									
0*r* Axis	PARAMETERS / MEDIUM	t_{fR}	μ_{TR}	λ_{TR}	T_{1R}	T_{2R}	r_f	μ_R	λ_R	R_1	R_2
	HOMOGENOUS	10	4	1.5	1	1.5	10	4	1.5	1	1.5
	INHOMOGENEOUS	26	4	1.167	3	3.5	26	4	1.167	3	3.5
	PDE (t,r)	$a_{00R}\cdot y_{00R}+a_{10R}\cdot y_{10R}+a_{20R}\cdot y_{20R}+a_{01R}\cdot y_{01R}+a_{02R}\cdot y_{02R}+a_{11R}\cdot y_{11R} = K_{yR}\cdot(\varphi_{0.00R}\cdot u_{0R}+\varphi_{1.00R}\cdot u_{1R}+\varphi_{2.00R}\cdot u_{2R})$									
	$\tilde{y}_{00R}(t,r)$	$K_{yR}\cdot(1-\frac{T_{1R}}{T_{1R}-T_{2R}}\cdot e^{-\frac{t}{T_{1R}}}-\frac{T_{2R}}{T_{2R}-T_{1R}}\cdot e^{-\frac{t}{T_{2R}}})\cdot(\frac{R_1}{R_1-R_2}\cdot e^{-\frac{r}{R_1}}-\frac{R_2}{R_2-R_1}\cdot e^{-\frac{r}{R_2}})$									

The notations of the intensity of the propagation ($y_{ij...}$) correspond with: $y_{ijP}=\frac{\partial^{i+j}y_{00P}}{\partial t^i\cdot\partial p^j}$, $y_{ijQ}=\frac{\partial^{i+j}y_{00Q}}{\partial t^i\cdot\partial q^j}$, $y_{ijR}=\frac{\partial^{i+j}y_{00R}}{\partial t^i\cdot\partial r^j}$, for i = 0, 1, 2 and j = 0, 1, 2, in each case, and the input signals ($u_{i...}$) correspond with $u_{i....}=\frac{d^iu_{i....}}{dt^i}$, for i = 0, 1, 2. The (a_{ijS}) coefficients, for $S = P$, then $S = Q$ and $S = R$, from the structure of the three PDE II (*t*,*s*), (where $s = p$, $s = q$ and $s = r$), have the expressions: $a_{00S} = 1$; $a_{10S} = T_{1S} + T_{2S}$; $a_{20S} = T_{1S} \cdot T_{2S}$; $a_{01S} = S_1 + S_2$; $a_{02S} = S_1 \cdot S_2$ and $a_{11S} = (T_{1S} +$

DOI: 10.7763/IJMO.2018.V8.650

+ T_{2S})·(S_1 + S_2). The structure parameters (T_{1S}, T_{2S}, S_1, S_2), that define the (a_{ijS}) from above, present phenomenological interpretations formally identical with the coefficients of the transfer functions of second order , where respectively (T_1 and T_2) are time constants, and (S_1 and S_2) are space constants (length, width, depth). It results that to each Cartesian axis, it corresponds a pair of time constants ($T_{1...}$; $T_{2...}$) and a pair of space constants ($S_{1...}$; $S_{2...}$), as it is formally presented in Fig. 2 and in Table I.

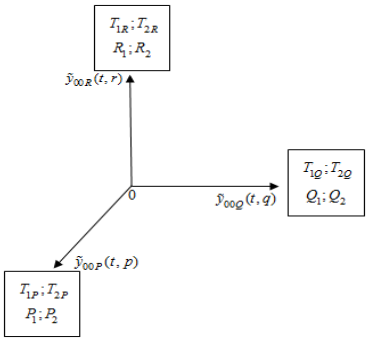

Fig. 2. The time constants and the space constants associated to Cartesian axes.

It is considered that for this propagation process (for example thermal) through dispersion, having different intensities on the three coordinate axes, the analytical solutions $y_{00P}(t, p)$, $y_{00Q}(t, q)$ and $y_{00R}(t, r)$ are not known. However, it is intended to use an approximating method of numerical simulation, which has closer results, consequence of a possible set of measurements that can reflect the reality accurate enough.

II. The Approximating Solutions

The approximating solutions $\tilde{y}_{00P}(t, p)$, $\tilde{y}_{00Q}(t, q)$ and $\tilde{y}_{00R}(t, r)$ necessary for the start of numerical integration (valid for unit step type input signal), are obtained through measurements, associated to procedures of expert type, being desirable to get as much closer as possible to the analytical solutions $y_{00P}(t, p)$, $y_{00Q}(t, q)$ and $y_{00R}(t, r)$. For these approximating solutions, the following usual expression is adopted

$$\tilde{y}_{00S}(t,s) = [K_{yS} \cdot F_{0TS}(t) \cdot F_{0S}(s)] * u_{0S}(t), \qquad (1)$$

which is singularized for each coordinate axis (respectively $S = P$; $S = Q$; $S = R$ and $s = p$, $s = q$ respectively $s = r$), from Table 1. Also, the notation "*" signifies the convolution product between the two functions depending on time (t).

With $u_{0S}(t)$ is notated the intensity of the propagation sources, localized in the origin of the Cartesian coordinate axes and oriented after each axis.

In the case of a perfect radial source (a spherical one), it is considered that $u_{0P}(t) = u_{0Q}(t) = u_{0R}(t)$, but in a more general case, the intensity of these sources can differ, respectively $u_{0P}(t) \neq u_{0Q}(t) \neq u_{0R}(t)$. In Fig. 3 it is considered that the exponential functions $F_{0TS}(t)$ are increasing ones, and $F_{0S}(s)$ are decreasing ones.

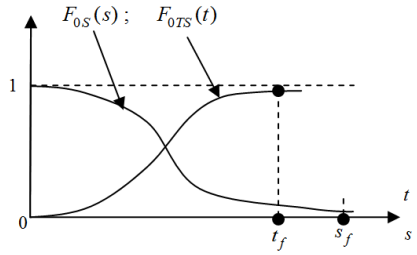

Fig. 3. The exponential functions $F_{0TS}(t)$ and $F_{0S}(s)$.

For the final values (t_f) and (s_f), it is considered that $F_{0TS}(t_f) \to 1$, respectively $F_{0S}(s_f) \to 0$. The (K_{yS}) coefficients, from (1) are proportionality constants, that for this paper are considered of unitary values.

Through the appropriate choice of these structure parameters, associated to each coordinate axis, respectively (T_{1P}, T_{2P}, P_1, P_2) for the ($0p$) axis, then (T_{1Q}, T_{2Q}, Q_1, Q_2) for the ($0q$) axis and finally (T_{1R}, T_{2R}, R_1, R_2) for the ($0r$) axis, it is intended to obtain a very close process' work description in relation to the measurement results gained through expert procedures.

For the non-periodical, exponentially increasing function $F_{0TS}(t)$, from (1) and from Fig. 3, it is chosen

$$F_{0TS}(t) = 1 - \frac{T_{1S}}{T_{1S} - T_{2S}} \cdot e^{-\frac{t}{T_{1S}}} - \frac{T_{2S}}{T_{2S} - T_{1S}} \cdot e^{-\frac{t}{T_{2S}}}, \qquad (2)$$

($S = P$; $S = Q$; $S = R$) and for the non-periodical, exponentially decreasing function $F_{0S}(s)$, also from (1) and from Fig. 3, it is chosen

$$F_{0S}(s) = \frac{S_1}{S_1 - S_2} \cdot e^{-\frac{s}{S_1}} - \frac{S_2}{S_2 - S_1} \cdot e^{-\frac{s}{S_2}}, \qquad (3)$$

($S = P$; $S = Q$; $S = R$), ($s = p$; $s = q$; $s = r$) with the remark that both functions, were proved to be appropriate, in numerous applications of the propagation phenomena.

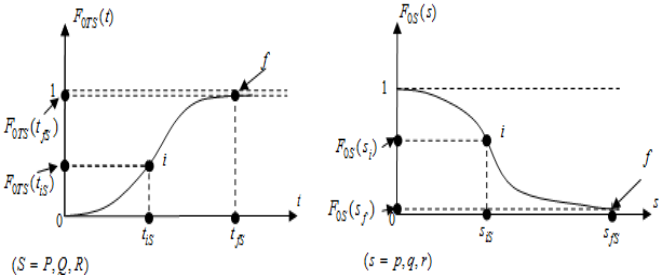

Fig. 4. The final values and the inflection points.

III. The Approximation of Time and Space Constants

The constants can differ, more or less, in relation to the three coordinate axes from Fig. 2. From the experimental curves, achieved through expert methods, it is approximated for each abscissa, the final values (t_f) and (s_f) from Fig. 3, as well as the values (t_{iS}) and (s_{iS}) for which these functions present inflections, respectively $\frac{d^2 F_{0TS}(t)}{dt^2} = 0$ and

$\frac{d^2F_{0S}(s)}{ds^2}=0$, as it is formally exemplified, for the point (i) from Fig. 4, with the indices $S = P$; $S = Q$; $S = R$, respectively $s = p$; $s = q$; $s = r$.

For the time constants, it is operated with the relations: $\mu_{TS}=\frac{t_{fS}}{T_{1S}+T_{2S}}$; $\lambda_{TS}=\frac{T_{2S}}{T_{1S}}$; $T_{1S}=\frac{t_{fS}}{\mu_{TS}\cdot(1+\lambda_{TS})}$; $T_{2S} = \lambda_{TS} \cdot T_{1S}$ as well as with the relation: $\frac{t_{iS}}{t_{fS}}=\frac{\lambda_{TS}\cdot\ln\lambda_{TS}}{\mu_{TS}\cdot(\lambda_{TS}^2-1)}$ (for $S = P, Q, R$). It is chosen $\lambda_{TS} > 1$, resulting: $\mu_{TS}=\frac{\lambda_{TS}\cdot\ln\lambda_{TS}}{\lambda_{TS}^2-1}\cdot\frac{t_{fs}}{t_{is}}$. It can also be established that $T_{1S}=\frac{\lambda_{TS}-1}{\lambda_{TS}\cdot\ln\lambda_{TS}}\cdot t_{iS}$, $T_{2S}=\frac{\lambda_{TS}-1}{\ln\lambda_{TS}}\cdot t_{iS}$. Formally identical, for the space constants, the following relations are also obtained: $\mu_S=\frac{s_{fS}}{S_1+S_2}$, $\lambda_S=\frac{S_2}{S_1}$, $S_1=\frac{s_{fS}}{\mu_S\cdot(1+\lambda_S)}$, $S_2=\lambda_S\cdot S_1$, $\frac{s_{iS}}{s_{fS}}=\frac{\lambda_S\cdot\ln\lambda_S}{\mu_S\cdot(\lambda_S^2-1)}$ (for $s = p, q, r$). It results $\mu_S=\frac{\lambda_S\cdot\ln\lambda_S}{\lambda_S^2-1}\cdot\frac{s_{fs}}{s_{is}}$ since $\lambda_S > 1$. It can be established that $S_1=\frac{\lambda_S-1}{\lambda_S\cdot\ln\lambda_S}\cdot s_{iS}$, $S_2=\frac{\lambda_S-1}{\ln\lambda_S}\cdot s_{iS}$. For numerous applications $t_{iS}\cong(0.1,0.20)\cdot t_{fs}$, and $s_{iS}\cong(0.1,0.20)\cdot s_{fs}$, where certainly the values for t_{fs} and s_{fs} are known.

If the propagation phenomena differ very much in relation to the Cartesian coordinate axes, it results that the final times (t_{fP}, t_{fQ} , t_{fR}), and the inflections values (t_{iP}, t_{iQ} , t_{iR}), can exhibit very different values. It results that the final propagation distances (s_{fP}, s_{fQ} , s_{fR}) and the associated ones to the inflection phenomena (s_{iP}, s_{iQ}, s_{iR}) can differ very much among each other. Consequently, according to previously presented equations, both the value of the time constants and of the space constants can have values even more different, in relation to the coordinate axes.

IV. Examples of Propagation in a Homogenous Medium

The propagation is considered identical on the three Cartesian coordinate axes from Figs. 1 and 2. Consequently, the homologous propagation constants will be equal, respectively the time constants: $T_{1P} = T_{1Q} = T_{1R}$ and $T_{2P} = T_{2Q} = T_{2R}$, also the space constants $P_1 = Q_1 = R_1$ and $P_1 = Q_1 = R_1$ $P_2 = Q_2 = R_2$. There are also considered: $t_{fS} = 10$; $S = P$; $S = Q$; $S = R$ (time units); $s_f = p_f = r_f = 10$ (length units); $\mu_{TS} = \mu_S = 4$; ($S = P$; $S = Q$; $S = R$), $\lambda_{TS} = \lambda_S = 1.5$; ($S = P$; $S = Q$; $S = R$). Finally, the time constants result as: $T_{1S}=\frac{t_{fS}}{\mu_{TS}\cdot(1+\lambda_{TS})}=0.1\cdot t_{fS}=1$; $T_{2S} = \lambda_{TS} \cdot T_{1S} = 1.5$, where $S = P$; $S = Q$; $S = R$, and the space constants (length): $S_1=\frac{s_f}{\mu_S\cdot(1+\lambda_S)}=0.1\cdot s_f=1$; $S_2 = \lambda_S \cdot S_1 = 1.5$, for $S = P, Q, R$ and $s = p, q, r$. Consequently, $T_{1S} = 1$; $T_{2S} = 1.5$; $S_1 = 1$; $S_2 = 1.5$.

The inflection abscissa can also be established as: $t_{iS}=\frac{\lambda_{TS}\cdot\ln(\lambda_{TS})}{\mu_{TS}\cdot(\lambda_{TS}^2-1)}\cdot t_{fS}=0.1216\cdot t_{fS}$ and $s_{iS}=\frac{\lambda_S\cdot\ln(\lambda_S)}{\mu_S\cdot(\lambda_S^2-1)}\cdot s_{fS}=0.1216\cdot s_{fS}$, with the remark that the time and the space (length) units are certainly different.

With the above data and according to (2), $F_{0TS}(t_{fS}) = 0.9962$ and $F_{0S}(t_{iS}) = 0.2592$ are calculated, and with relation (3) $F_{0S}(s_f) = 0.0037$ and $F_{0S}(s_i) = 0.7407$ are calculated, as it is formally presented in Fig. 4, too. The numerical simulation inside of this medium is operated on the spatial curve of a spiral [8,9], defined through the system of parametric equations:

$$p = p(t) = \rho\cdot\cos\frac{2\cdot\pi}{T_\rho}\cdot t \tag{4}$$

$$q = q(t) = \rho\cdot\sin\frac{2\cdot\pi}{T_\rho}\cdot t\,, \tag{5}$$

$$r = r(t) = \frac{\delta r}{T_\rho}\cdot t\,, \tag{6}$$

where (ρ) and (T_ρ) correspond with the radius of the spiral, respectively with the period of a complete revolution, and (δr) is the step of the spiral.

The dedicated MATLAB program CPARAM5(6) is used based on the method of the matrix of partial derivatives of the state vector ($\boldsymbol{M_{pdx}}$), associated with Taylor series, [3], using for the start of the calculus the approximating solutions $\tilde{y}_{00S}(t,s)$, from (1). Other initialization parameters than the previously mentioned ones, are: $\rho = 0.5$; $\delta r = 1$; $T_\rho = 1.2$; $K_y = 1$; $\theta = 0$; $\Delta t = 0.01$; $\Delta\theta = \Delta t \cdot 100$. The extraction of integration results on the three coordinate axes, is made simultaneously in the moments $t = n\cdot\frac{T_\rho}{12}$, for $n = 0, 1,2,...,12$, as it is presented in Tables 2, 3 and 4, for $T_1 = 1$; $T_2 = 1.5$; $S_1 = 1$; $S_2 = 1.5$; $\rho = 0.5$; $T_\rho = 1.2$; $\delta r = 1$; $K_y = 1$; $u_0 = 10$ and the extraction step $\Delta\theta=\frac{T_\rho}{12}$. It is remarked that $p(t)$ and $q(t)$ present non-periodical behaviors with amplitudes of (±5), and $r(t)$ is an increasing linear variable. The exponential solutions $y_P(t,p)$ and $y_Q(t,q)$ present small periodical components, and the exponential solution $y_R(t,r)$, after reaching a maximum, is progressively decreasing until a value practically negligible.

Table II corresponds to the first period (T_ρ), meaning ($0 \le t \le T_\rho$), with the (r) increasing abscissa, from $t = 0$; $r = 0$, until $t = t_f = T_\rho$, respectively $r=\frac{\delta r}{T_\rho}\cdot T_\rho=1$. Table 3 is referring to the third period, ($3 \cdot T_\rho \le t \le 4 \cdot T_\rho$), with the increasing abscissa (r), from $t = 3 \cdot T_\rho = 3.6$; $r = 3$, until $t = 4 \cdot T_\rho = 4.8$, respectively $r = 4$. Table 4 contains the tenths period, respectively ($10 \cdot T_\rho \le t \le 11 \cdot T_\rho$), with the increasing abscissa (r), from $t = 10 \cdot T_\rho = 12$; $r = 10$, until $t = 11 \cdot T_\rho = 13.2$, and $r = 11$.

The final result $y(t,p,q,r)$, corresponds to a "space-temporal hypotenuse", according to the obvious relation:

$$y(t, p, q, r) = \sqrt{y_P^2(t,p)+y_Q^2(t,q)+y_R^2(t,r)}\,, \qquad (7)$$

as passing back from the parametric coordinates (4), (5), (6), that define the spiral, to the Cartesian coordinates. It is remarked that while advancing in time, respectively from the Table 2, to Table 3, then Table 4, the values of y (t, p, q, r) from (7), are increasing progressively more slowly, so as, in Table 4 practically they get steady between (13.650,13.690). Hence, it results that the final solution y (t, p, q, r) obviously presents an exponential evolution, too, increasing in transitory regime (Table II), and then practically stabilized in stationary regime (Table IV).

TABLE II: SIMULATION RESULTS CORRESPONDING TO THE FIRST PERIOD

t	0	$\frac{T_p}{12}$	$2\cdot\frac{T_p}{12}$	$3\cdot\frac{T_p}{12}$	$4\cdot\frac{T_p}{12}$	$5\cdot\frac{T_p}{12}$	$6\cdot\frac{T_p}{12}$	$7\cdot\frac{T_p}{12}$	$8\cdot\frac{T_p}{12}$	$9\cdot\frac{T_p}{12}$	$10\cdot\frac{T_p}{12}$	$11\cdot\frac{T_p}{12}$	$12\cdot\frac{T_p}{12}$
φ^0	0	30	60	90	120	150	180	210	240	270	300	330	360
p	0.5	0.433	0.25	$-8\cdot10^{-8}$	− 0.25	− 0.433	− 0.5	− 0.433	− 0.255	$5\cdot10^{-7}$	0.25	0.433	0.5
q	0	0.25	0.439	0.5	0.433	0.25	-10^{-7}	− 0.25	− 0.433	− 0.5	− 0.433	− 0.25	$5\cdot10^{-7}$
r	0	$8\cdot10^{-2}$	0.166	0.25	0.333	0.416	0.5	0.583	0.666	0.75	0.833	0.916	1
y_P	0	0.03	0.117	0.254	0.420	0.603	0.811	1.063	1.362	1.667	1.919	2.137	2.382
y_Q	0	0.03	0.113	0.238	0.407	0.623	0.866	1.098	1.318	1.561	1.858	2.207	2.544
y_R	0	0.03	0.118	0.249	0.415	0.605	0.811	1.026	1.243	1.458	1.665	1.862	2.046
y	0	0.0533	0.201	0.4288	0.718	1.057	1.438	1.841	2.267	2.709	3.1483	3.593	4.042

TABLE III: SIMULATION RESULTS CORRESPONDING TO THE THIRD PERIOD

t	3.6	3.7	3.8	3.9	4	4.1	4.2	4.3	4.4	4.5	4.6	4.7	4.8
φ^0	1080	1110	1140	1170	1200	1230	1260	1290	1320	1350	1380	1410	1440
p	0.5	0.433	0.25	10^{-6}	− 0.25	− 0.433	− 0.5	− 0.433	− 0.25	-10^{-6}	0.25	0.433	0.5
q	10^{-6}	0.25	0.433	0.5	0.433	0.250	10^{-6}	− 0.25	− 0.433	− 0.5	− 0.433	− 0.25	10^{-6}
r	3	3.083	3.166	3.25	3.333	3.41	3.5	3.58	3.666	3.75	3.83	3.91	4
y_P	7.32	7.55	7.919	8.17	8.131	7.96	7.937	8.14	8.49	8.728	8.64	8.43	8.37
y_Q	7.82	7.804	7.667	7.65	7.873	8.229	8.475	8.41	8.22	8.174	8.37	8.71	8.94
y_R	2.39	2.32	2.250	2.17	2.101	2.027	1.954	1.881	1.809	1.739	1.67	1.60	1.536
y	10.98	11.108	11.25	11.412	11.51	11.63	11.775	11.855	11.95	12.08	12.14	12.23	12.34

TABLE IV: SIMULATION RESULTS CORRESPONDING TO THE TENTHS PERIOD

t	12	12.1	12.2	12.3	12.4	12.5	12.6	12.7	12.8	12.9	13	13.1	13.2
φ^0	3600	3630	3660	3690	3720	3750	3780	3810	3840	3870	3900	3930	3960
p	0.5	0.433	0.25	$-3\cdot10^{-5}$	− 0.25	− 0.433	− 0.5	− 0.433	− 0.25	$3\cdot10^{-5}$	0.25	0.433	0.5
q	$2\cdot10^{-5}$	0.25	0.433	0.5	0.433	0.25	$-3\cdot10^{-5}$	− 0.25	− 0.433	− 0.5	− 0.433	− 0.25	$3\cdot10^{-5}$
r	10	10.083	10.166	10.25	10.333	10.41	10.50	10.58	10.666	10.75	10.833	10.916	11
y_P	9.35	9.497	9.81	9.992	9.811	9.5	9.359	9.50	9.812	9.994	9.813	9.50	9.361
y_Q	9.99	9.809	9.498	9.357	9.50	9.811	9.993	9.812	9.501	9.36	9.501	9.814	9.995
y_R	0.0372	0.035	$3\cdot10^{-2}$	$3\cdot10^{-2}$	$3\cdot10^{-2}$	0.028	$2\cdot10^{-2}$	$2\cdot10^{-2}$	$2\cdot10^{-2}$	$2\cdot10^{-2}$	$2\cdot10^{-2}$	0.020	$2\cdot10^{-2}$
y	13.687	13.653	13.654	13.689	13.656	13.657	13.691	13.658	13.658	13.693	13.659	13.660	13.694

The radius (ρ) of the spiral is (arbitrary) chosen sub-unitary as $\rho = 0.5$, in order to maintain the spiral evolution, inside the limits: $p_f = 1$; $q_f = 1$; $r_f = 1$. In the initialization instructions, the corresponding ones result: $T_{1PA} = T_{1P}$; $T_{2PA} = T_{2P}$; $T_{1QA} = T_{1Q}$; $T_{2QA} = T_{2Q}$; $T_{1RA} = T_{1R}$; $T_{2RA} = T_{2R}$; $S_{1PA} = P_1$; $S_{2PA} = P_2$; $S_{1QA} = Q_1$; $S_{2QA} = Q_2$; $S_{1RA} = R_1$; $S_{2RA} = R_2$. Also $p_A = p$; $q_A = q$; and $r_A = r$.

The intensity of supply sources is big enough, respectively [$u_{0P} = u_{0Q} = u_{0PR} = u_{EXTA} = 10$], in order to avoid the much sub-unitary results.

In Fig. 5 the solution $y(t,p,q,r)$ is presented, for the thirteen periods of the simulation. The data associated to the Tables II, III, IV are included in this figure.

The graph from Fig. 5 is a 3D representation of the y solution for the homogenous medium that highlights in an intuitive manner the considered spiral. From Fig. 5, it can be remarked that the steady state regime appears after the first seven periods.

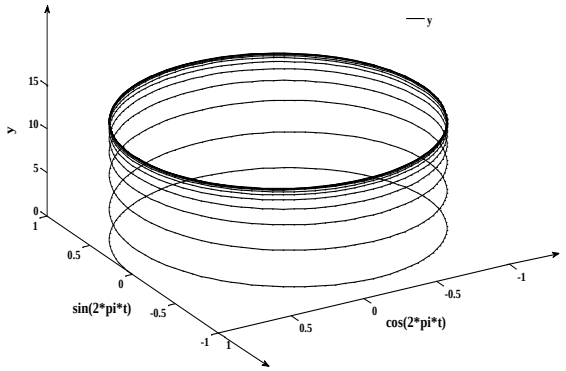

Fig. 5. The evolution of the y solution for homogenous medium.

V. EXAMPLE OF PROPAGATION IN AN INHOMOGENEOUS

The propagation is considered different on the three Cartesian coordinate axes from Fig. 2. It is highlighted the inhomogeneity of the propagation medium through different values of the time constants ($T_{1...}$; $T_{2...}$) and of the space constants ($S_{1...}$; $S_{2...}$), through the initializing instructions from the new program CPARAM7(8), respectively: $T_{1PA} = 1$; $T_{2PA} = 1.5$; $T_{1QA} = 2$; $T_{2QA} = 2.5$; $T_{1RA} = 3$; $T_{2RA} = 3.5$; $S_{1PA} = 1$; $S_{2PA} = 1.5$; $S_{1QA} = 2$; $S_{2QA} = 2.5$; $S_{1RA} = 3$; $S_{2RA} = 3.5$; $\rho = 0.5$; $\delta r = 1$; $T_\rho = 1.2$; $\lambda_{TQ} = \frac{T_{2Q}}{T_{1Q}} = 1.25$; $\lambda_Q = \frac{Q_2}{Q_1} = 1.25$; $\lambda_{TR} = \frac{T_{2R}}{T_{1R}} = 1.167$; $\lambda_R = \frac{R_2}{R_1} = 1.167$; $t_{fQ} = \mu_{TQ} \cdot (T_{1Q} + T_{2Q}) = 18$; $t_{fR} = \mu_{TR} \cdot (T_{1R} + T_{2R}) = 26$; $q_f = \mu_Q \cdot (Q_1 + Q_2) = 18$; $r_f = \mu_R \cdot (R_1 + R_2) = 26$. For the first period, the simulation results are presented in Table V.

TABLE V: SIMULATION RESULTS CORRESPONDING TO THE FIRST PERIOD

t	0	$\frac{T_p}{12}$	$2\cdot\frac{T_p}{12}$	$3\cdot\frac{T_p}{12}$	$4\cdot\frac{T_p}{12}$	$5\cdot\frac{T_p}{12}$	$6\cdot\frac{T_p}{12}$	$7\cdot\frac{T_p}{12}$	$8\cdot\frac{T_p}{12}$	$9\cdot\frac{T_p}{12}$	$10\cdot\frac{T_p}{12}$	$11\cdot\frac{T_p}{12}$	$12\cdot\frac{T_p}{12}$
		0.1	0.2	0.3	0.4	0.5	0.6	0.7	0.8	0.9	1.0	1.1	1.2
φ^0	0	30	60	90	120	150	180	210	240	270	300	330	360
p	0.5	0.433	0.25	-10^{-7}	− 0.25	− 0.433	− 0.5	− 0.433	− 0.25	10^{-7}	0.25	0.433	0.5
q	0	0.25	0.433	0.5	0.433	0.25	-10^{-7}	− 0.25	− 0.433	− 0.5	− 0.433	− 0.25	10^{-7}
r	0	0.083	0.166	0.25	0.333	0.416	0.5	0.583	0.666	0.75	0.833	0.916	1
y_P	0	0.03	0.117	0.254	0.420	0.603	0.811	1.063	1.362	1.667	1.92	2.137	2.38
y_Q	0	0.009	0.037	0.08	0.134	0.214	0.301	0.396	0.497	0.608	0.733	0.871	1.01
y_R	0	0.004	0.018	0.04	0.07	0.106	0.15	0.20	0.254	0.313	0.377	0.445	0.516
y	0	0.032	0.124	0.27	0.449	0.649	0.878	1.15	1.472	1.802	2.09	2.35	2.64

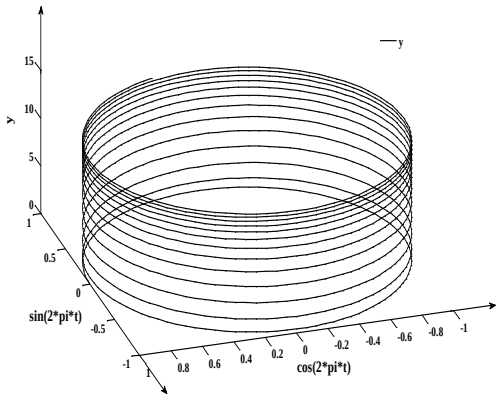

Fig. 6. The evolution of the y solution for inhomogeneous medium.

In the Fig. 6, the solution $y(t,p,q,r)$ is presented, for the thirteen periods of the simulation. In this case, also, the graph from Fig. 6 is a 3D representation of the y solution, but for the

inhomogeneous medium. The tendency to steady state regime is obvious in the upper part of the graph, where evolution of the *y* solution is much slower than in the intermediary, respectively in the lower part of the graph. In Fig. 7, a comparative graph between the *y* solutions for the two mediums (homogenous and inhomogeneous) is presented.

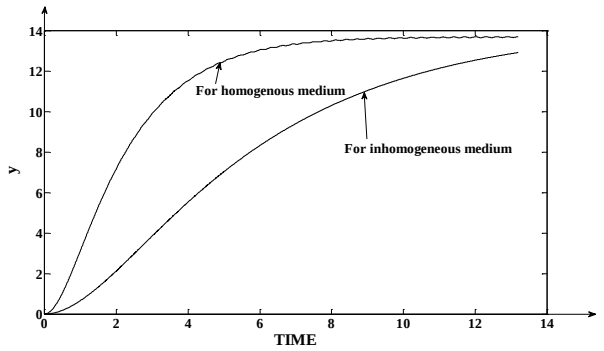

Fig. 7. The *y* solutions for both homogeneous and inhomogeneous mediums.

From Fig. 7 it results a higher inertia of the propagation phenomenon in the case of the inhomogeneous medium comparing with the homogeneous medium case.

VI. Conclusion

The paper presents, a procedure of numerical simulation, oriented on spatial curves (for example spirals), for distributed parameter propagation processes. The analogical model of these processes is expressed through systems of three equations with partial derivatives of second order with, respectively PDE II(*t*,*p*), PDE II(*t*,*q*) and PDE II(*t*,*r*), where the variables (*p*), (*q*) and (*r*) belong to the Cartesian coordinate axes (0*p*), (0*q*) respectively (0*r*). The form of these three equations with partial derivatives is exemplified in Table 1, and the expressions of the (a_{ijS}) coefficients are considered dependent on the time constants (T_{1S}; T_{2S}) and on the space constants (S_1; S_2) shown in the INTRODUCTION. For both mediums, with homogenous and inhomogeneous propagation, the same initial spatial curve is associated, respectively the spiral. It is defined through the parametric system of equations (4), (5), (6), having the radius (ρ), the period of a complete rotation T_ρ and the gradient (coefficient) of increasing ($\frac{\delta r}{T_\rho}$) in relation to time. The return from the parametric coordinates, to the Cartesian coordinates is operated through relation (7). The example of propagation in a homogenous medium is studied through a dedicated program CPARAM 5(6). For the spiral, the radius $\rho = 0.5$, the period $T_\rho = 1.2$ and the step $\delta r = 1$ on the 0*r* axis are considered. The final solution $y(t,p,q,r)$ can be interpreted as a spatial-temporal propagation resultant signal, (radiant energy, temperature, pressure, chemical concentration) than can be simultaneously obtained from the solution of three equations with partial derivatives, disposed on the Cartesian coordinate axes, having identical propagation parameters. It is considered the same intensity of the propagation sources, associated to the Cartesian coordinate axes, respectively $u_{0P}(t) = u_{0Q}(t) = u_{0R}(t) = u_{EXTA}(t) = 10$. The example of propagation in a inhomogeneous medium is studied through a dedicated program CPARAM 7(8).

References

[1] T. Coloşi, M. Abrudean, M.-L. Ungureşan, and V. Mureşan, *Examples of Numerical Simulation for Systems with Distributed and Lumped Parameters through the Mpdx Method with Approximating Solutions*, p. 98, 2013, UTPRESS Publishing House.

[2] T. Coloşi, M. Abrudean, M. L. Ungureşan, and V. Mureşan, "Cascade PID control of some processes with distributed parameters through (Mpdx) method with approximating solutions," *in Proc. ICPS'13 (Convergence of Information Technologies and Control Methods with Power Systems)*, 2013, Cluj-Napoca, Romania, pp. 21-28.

[3] T. Coloşi, M. Abrudean, M.-L. Ungureşan, and V. Mureşan, *Numerical Simulation of Distributed Parameters Processes*, 363 pages, 2013, SPRINGER Publishing house.

[4] M. Krstic, "Systematization of approaches to adaptive boundary control of PDEs," *International Journal of Robust and Nonlinear Control*, 2006, vol. 16, pp. 801-818.

[5] W. S. Levine, *The Control Handbook, Second Edition: Control System Applications, Second Edition (Electrical Engineering Handbook)*, 2010, Publisher: CRC Press, 2 edition.

[6] H.-X. Li and C. Qi, *Spatio-Temporal Modeling of Nonlinear Distributed Parameter Systems: A Time/Space Separation Based Approach*, 2011, p. 194, Springer Publishing House. 1st Edition.

[7] J. Love, *Process Automation Handbook*, Publisher: Springer Publishing House, 2007.

[8] V. Mureşan and M. Abrudean, "Temperature modelling and simulation in the furnace with rotary hearth," *in Proc. 2010 IEEE AQTR 2010–17th edition*, 2010, Cluj-Napoca, Romania, pp. 147-152.

[9] V. Mureşan, M. Abrudean, M.-L. Ungureşan and T. Coloşi, "Control of the Blunting Process of the Residual Water from a Foundry," *in SACI IEEE 7th International Symposium on Applied Computational Intelligence and Informatics*, 2012, Timişoara, Romania.

Vlad Mureşan is an associate professor with Technical University of Cluj-Napoca, Automation Department, Romania.

His research interests are mathematical modeling and numerical simulation of distributed parameter processes, industrial plant control, isotope separation processes, advance control of the metallurgical processes, intelligent control, biomedical processes etc.

He has 105 papers published in journals or communicated at international conferences, as well as 7 books and 10 research contracts where I was the manager or member in the research team.

Iulia Clitan graduated at the Automation and Computer Science Faculty and she completed her master's degree of advanced process control at the Technical University of Cluj-Napoca, Romania. She received her doctorate in systems engineering at the same University. Her research interests are industrial process control and biomedical engineering. She is currently a lecturer at the Automation Department from the Technical University of Cluj-Napoca.

Tiberiu Coloşi was graduated 1957, with honors, from the Electro Technical School of the Politechnical Institute in Timişoara.

Between1957-1965 he worked as an electroenergetic engineer at the Coal Company Valea Jiului.

Starting 1965 and until 2003 he taught automatics and electronics at the Faculty for Automatics and Computers of the Technical University of Cluj-Napoca.

Since 2003 he is a consulting professor at the same University.

He is a PhD in automatics since 1972 and a full professor since 1978.

He was a fellow of the Alexander von Humboldt Foundation (1974-1975; 2000) at Institut fuer Allgemeine und Theoretische Elektrotechnik der Universitaet Erlangen-Nuernberg.

He is a correspondent member of the Romanian Academy for Technical Sciences.

Domains of interest: Systems theory, Industrial processes control, Numerical simulation of processes with distributed parameters.

Mihail Ioan Abrudean is a professor with Technical University of Cluj-Napoca, Automation Department, Romania

His research interests are mathematical modeling and numerical simulation with distributed parameter processes, robust nonlinear control of isotope separation columns, robust-predictive control of isotope separation columns etc.

He has 253 papers published in journals or communicated at international conferences, 5 patents, 15 books and 82 research contracts where I was the manager or member in the research team.

Mihaela-Ligia Ungureşan is an associate professor with Technical University of Cluj-Napoca, Physics and Chemistry Department, Romania

Her research interests are chemical kinetics of rapid reactions, isotopic exchange reactions, modeling and simulation of physical-chemical processes, synthesis of chemical compound marked with stable isotopes etc.

She has 118 papers published in journals or communicated at international conferences, as well as the fifteen books and 30 research contracts where I was the manager or member in the research team.

Andrei Florin Clitan is a lecturer at the Technical University of Cluj-Napoca, Romania. He is part of the Railways, Roads and Bridges Department since 2011. He obtained his PhD in civil engineering in 2012 at the same University, Faculty of Constructions. He graduated first of his class in 2009 the Faculty of Construction, Domain of Railways, Roads and Bridges. Currently his activities are divided between teaching and research. Main research domains are traffic, sustainable transportation and road